

HIGH RESOLUTION ROTATION CURVES OF LOW SURFACE BRIGHTNESS GALAXIES

R.A. SWATERS¹, B.F. MADORE², M. TREWHELLA³

Accepted for publication in ApJ Letters

ABSTRACT

High resolution H α rotation curves are presented for five low surface brightness galaxies. These H α rotation curves have shapes different from those previously derived from H I observations, probably because of the higher spatial resolution of the H α observations. The H α rotation curves rise more steeply in the inner parts than the H I rotation curves and reach a flat part beyond about two disk scale lengths. With radii expressed in optical disk scale lengths, the rotation curves of the low surface brightness galaxies presented here and those of HSB galaxies have almost identical shapes. Mass modeling shows that the contribution of the stellar component to the rotation curves may be scaled to explain most of the inner parts of the rotation curves, albeit with high stellar mass-to-light ratios. On the other hand, well fitting mass models can also be obtained with lower contributions of the stellar disk. These observations suggest that the luminous mass density and the total mass density are coupled in the inner parts of these galaxies.

Subject headings: galaxies: halos — galaxies: kinematics and dynamics — galaxies: structure

1. INTRODUCTION

The rotation curves of high surface brightness (HSB) spiral galaxies rise fairly steeply to reach an extended, approximately flat part, well within the optical disk (Bosma 1978, 1981a,b; Rubin, Ford, & Thonnard 1978, 1980). The discovery that the rotation curves of these galaxies are more or less flat out to one or two Holmberg radii has been one of the key pieces of evidence for the existence of dark matter outside the optical disk (see also van Albada et al. 1985). Within the optical disk, the observed rotation curves can in most cases be explained by the stellar components alone (Kalnajs 1983; Kent 1986).

The rotation curves of so-called low surface brightness (LSB) galaxies have been studied only recently (de Blok, McGaugh, & van der Hulst 1996, hereafter BMH; see also Pickering et al. 1997). These rotation curves, derived from H I observations, were found to rise more slowly than those of HSB galaxies of the same luminosity, if the radii are measured in kpc. At the outermost measured point, they were often still rising. McGaugh & de Blok (1998) noted that, with radii expressed in disk scale lengths, the rotation curve shapes of LSB and HSB galaxies become more similar, but not necessarily identical. Based on mass modeling of these H I rotation curves, de Blok & McGaugh (1997, hereafter BM) concluded that LSB galaxies were dominated by dark matter and that the contribution of the stellar disk to the rotation curve, even if scaled to its maximum possible value, could not explain the observed rotation curve in the inner parts.

The H I rotation curves of LSB galaxies have received a great deal of attention, because they provide additional constraints on theories of galaxy formation and evolution, and dark halo structure (e.g., Dalcanton, Spergel, & Summers 1997; Mihos, Mc-

Gaugh, & de Blok 1997; Hernandez & Gilmore 1998; Kravtsov et al. 1998; McGaugh & de Blok 1998). Unfortunately, most of the galaxies studied in BMH and BM are only poorly resolved, making their results sensitive to the effects of beam smearing. For five of the galaxies in their sample, high resolution H α rotation curves, which have been obtained in order to eliminate beam smearing and to investigate the rotation curve shapes in the inner parts of LSB galaxies, are presented in this Letter.

2. SAMPLE, OBSERVATIONS AND DATA REDUCTION

The galaxies presented here were selected from the sample of LSB galaxies of BMH. Only galaxies were chosen that satisfied the criteria given in BM to define their useful rotation curves. An overview of the properties of the galaxies is given in Table 1, which lists the name of the galaxy (1), the adopted distance in Mpc, for $H_0 = 75 \text{ km s}^{-1} \text{ Mpc}^{-1}$ (2), the central surface brightness in mag arcsec $^{-2}$ (3), the disk scale length in kpc (4), the inclination angle (5), the position angle (6), the absolute magnitude (7) and the systemic velocity (8).

The observations were carried out at Palomar Observatory with the 200'' Hale telescope⁴, on November 20 1998. The FWHM velocity resolution was 54 km s^{-1} , the pixel size in the spatial direction was $0.5''$. Each galaxy spectrum consisted of a single 1800s exposure. The slit was oriented along the major axis, at the position angle derived by BMH (see Table 1). Despite their low surface brightnesses, all galaxies showed up clearly on the slit-viewing monitor. The slit could therefore accurately be aligned with the center of the galaxy by eye. The data were reduced using standard procedures in IRAF and the resulting H α position-velocity diagrams are presented in Fig. 1.

¹Kapteyn Astronomical Institute, University of Groningen, The Netherlands and Department of Terrestrial Magnetism, Carnegie Institution of Washington, Washington DC 20015, USA

²Observatories of the Carnegie Institution of Washington and NASA/IPAC Extragalactic Database, California Institute of Technology, Pasadena CA 91125, USA

³Infrared Processing and Analysis Center, California Institute of Technology, Pasadena CA 91125, USA

⁴The Palomar 200'' telescope is operated in a joint agreement among the California Institute of Technology, the Jet Propulsion Laboratory and Cornell University

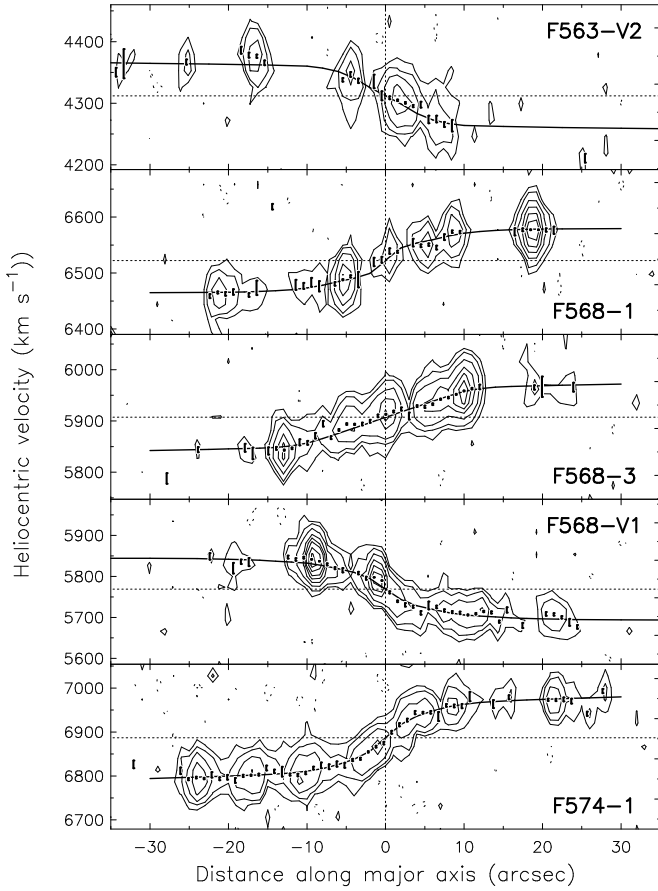


FIG. 1.— $\text{H}\alpha$ position-velocity diagrams for the five LSB galaxies, binned to $1''$. Contour levels are at $-2, 2, 4, 8, 16, 24, 32$ times the r.m.s. noise. The dots with errorbars give the radial velocities with the formal errors as derived from Gaussian fits to the velocity profiles. The solid lines represent the rotation curves, derived as described in section 3. The vertical dotted line indicates the galaxy center, the horizontal dotted lines denotes the heliocentric systemic velocities.

TABLE 1
PROPERTIES OF THE GALAXIES^a

Name	D (Mpc)	μ_0^B (mag/ $''''$ $^{-2}$)	h (kpc)	i ($^{\circ}$)	P.A. ($^{\circ}$)	M_B (mag)	v_{sys}^b (km s $^{-1}$)
(1)	(2)	(3)	(4)	(5)	(6)	(7)	(8)
F563-V2	61	22.1	2.1	29	148	-18.2	4310 ± 4
F568-1	85	23.8	5.3	26	13	-18.1	6524 ± 6
F568-3	77	23.1	4.0	40	169	-18.3	5911 ± 3
F568-V1	80	23.3	3.2	40	136	-17.9	5769 ± 7
F574-1	96	23.3	4.3	65	90 ^c	-18.4	6889 ± 6

^a Data from de Blok et al. (1996) and de Blok & McGaugh (1997).

^b This Letter.

^c A P.A. of 90° was used, derived from the optical image in BMH.

3. THE HIGH RESOLUTION ROTATION CURVES

To derive the rotation curves, we started by making Gaussian fits to the line profiles at each position along the major axis to obtain the radial velocities. These fits and their errors are overlayed on the $\text{H}\alpha$ position-velocity diagram in Fig. 1. The positions of the galaxy centers were determined from the peak of the continuum light along the slit. All galaxies were suffi-

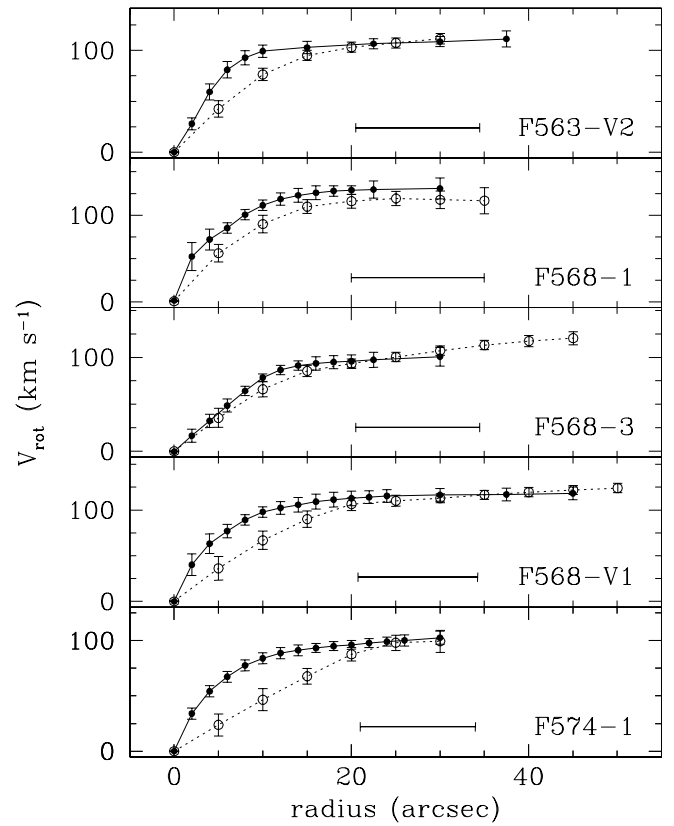


FIG. 2.— The high resolution $\text{H}\alpha$ rotation curves (filled circles, solid lines) and the H I rotation curves from BMH (open circles, dotted lines). The horizontal bar shows the FWHM beam size of the H I observations.

ciently bright to allow to determine the position of the center along the slit with an accuracy of better than $1''$.

To obtain a larger radial coverage of the rotation curves, the $\text{H}\alpha$ data were combined with the H I data presented in BMH. To this end, the derived $\text{H}\alpha$ velocities were plotted on the H I position-velocity diagrams. Both sets of data were found to agree well with each other if the effects of beam smearing on the H I data are taken into account (cf. Swaters 1999). Therefore, we have used the H I data to determine rotation velocities beyond radii where we found $\text{H}\alpha$ emission. Note that in most cases the H I extends only little beyond the $\text{H}\alpha$. Next, the rotation curves derived for the approaching and the receding sides were combined. The $\text{H}\alpha$ points were sampled every $2''$, the H I points every $7.5''$ (approximately two points per beam). The errors on the rotation velocities were estimated from the differences between the two sides and the uncertainties in the derived velocities. We will refer to these rotation curves as the high resolution rotation curves (HRC).

The derived HRCs are shown in Fig. 2 together with the H I rotation curves presented in BM. Probably because BM did not correct for beam smearing, the H I rotation curves systematically underestimate the inner slopes of the rotation curves, especially for F568-V1 and F574-1. Both these galaxies have a central depression in the H I distribution, as can be seen in the H I maps presented in BMH. The spatial smearing of H I from

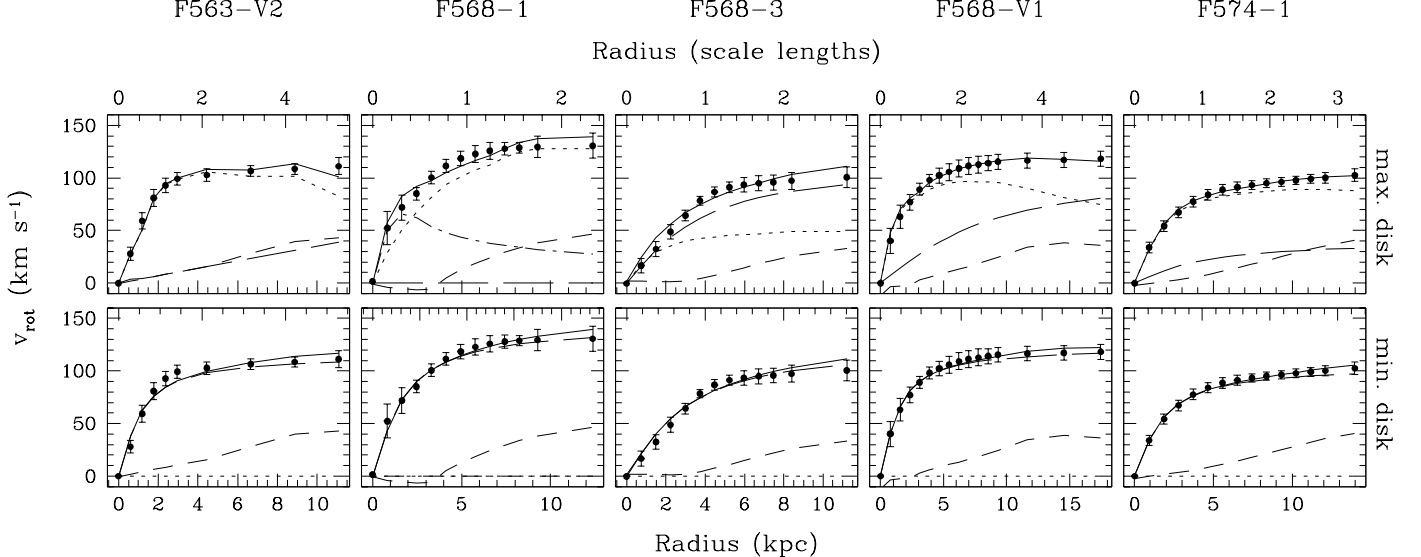


FIG. 3.— Mass models fitted to the high resolution rotation curves. The top panels give maximum disk fits, the bottom panels give fits with a stellar mass-to-light ratio of zero. The dotted line represents the contribution of the stellar disk to the rotation curve, the dashed line the contribution of the gas, the long-dashed line represents the dark halo, and the full line represented the total model rotation curve. For F568-1, the dot-dashed line represents the contribution of the central component to the rotation curve.

larger radii into the observed central depression leads to an apparent solid body-like rotation curve, in particular for the highly inclined galaxy F574-1.

4. MASS MODELING

For the mass modeling presented here we have used the same parameters for the thickness of the gaseous and stellar disks as BM have done. The stellar disk was assumed to have a vertical sech^2 distribution, with a scale height $z_0 = h/6$. R -band light profiles, presented in de Blok, van der Hulst, & Bothun (1995) and BMH, were used to calculate the contribution of the stellar disk to the rotation curve. The H I was assumed to reside in an infinitely thin disk. The only difference with the mass models presented in BM is that we have decomposed the light profile of F568-1 into a disk and a central component, and fitted these components to the rotation curve separately. In the other galaxies no significant central component is present. For the dark matter component a pseudo-isothermal halo was used, following BM, which has a rotation curve given by:

$$v_{\text{halo}}^2(r) = 4\pi G \rho_0 r_c^2 \left[1 - \frac{r_c}{r} \arctan \left(\frac{r}{r_c} \right) \right],$$

where r_c is the halo core radius and ρ_0 is the central density.

One of the major uncertainties in fitting mass models to rotation curves, in absence of an independent measurement of the stellar mass-to-light ratio Υ_* , is the uncertainty in the contribution of the stellar disk to the rotation curve. However, lower and upper limits on Υ_* , and hence on the dark matter content, can be obtained by assuming that the contribution of the stellar disk to the rotation curve is either minimal or maximal.

In the maximum disk mass models, the contribution of the stellar disk to the rotation curve is scaled to explain most of the inner parts of the rotation curve. The resulting rotation curve fits are shown in the top panel of Fig. 3. What immediately strikes the eye is that, in contrast with the findings of BM,

TABLE 2
MASS MODEL PARAMETERS

LSBC name	max. disk			no disk	
	Υ_* $M_\odot / L_{R,\odot}$	r_c kpc	ρ_0 $M_\odot \text{pc}^{-3}$	r_c kpc	ρ_0 $M_\odot \text{pc}^{-3}$
F563-V2 ^a	5.4	0.94	0.283
F568-1 ^b	17.2	1.5	0.181
F568-3	1.5	3.0	0.027	2.5	0.48
F568-V1	9.3	6.7	0.005	1.2	0.188
F574-1	3.7	3.4	0.003	1.5	0.92

^a No R -band data are available, mass modeling is based B -band data.

^b For F568-1 a central component was fitted separately, which has $\Upsilon_{\text{bulge}} = 14.4$ in the maximum disk fit.

inner parts of the rotation curves can be explained almost entirely by the contribution of the stellar disk in all of these LSB galaxies, with the exception of F568-3. The dark halo parameters (see Table 2) are ill-defined for most galaxies in our sample, because most of the HRCs do not extend to large radii. Nonetheless, it is clear that in these maximum disk fits the contribution of the dark halo will only become important outside the optical disk, as is also the case for HSB galaxies.

The required stellar mass-to-light ratios for the maximum disk fits (listed in Table 2), may be high, up to 17 in the R -band. Most of these are well outside the range of what current population synthesis models predict (e.g., Worthey 1994). If these high values of Υ_* are to be explained solely by a stellar population, the stellar content and the processes of star formation in LSB galaxies need to be very different from those in HSB galaxies. Alternatively, these high mass-to-light ratios may indicate the presence of an additional baryonic component that is associated with the disk, as has been suggested by e.g. Pfenniger, Combes, & Martinet (1994). On the other hand, the fact that stellar disk can be scaled to explain the observed rotation curve may simply reflect the possibility that the luminous and dark mass have a similar distribution within the optical galaxy.

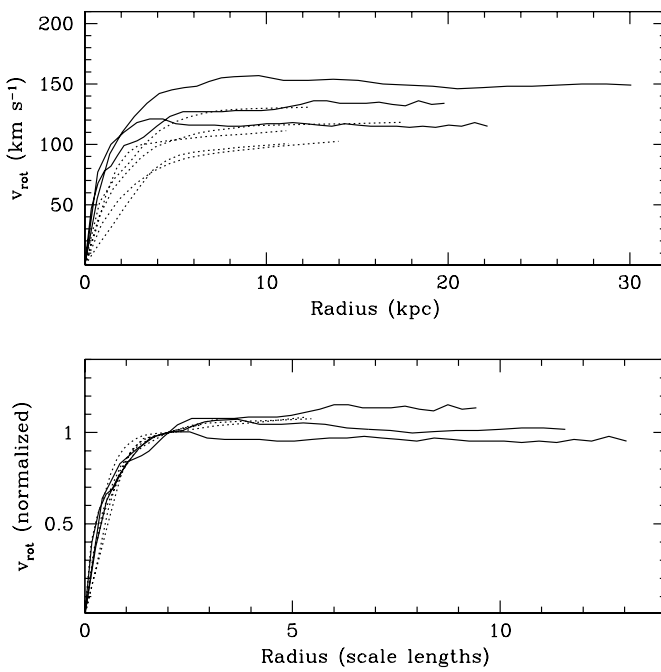


FIG. 4.— Rotation curves of the five LSB galaxies (dotted lines) compared to the rotation curves of three typical late-type HSB spiral galaxies from Begeman (1987): NGC 2403 ($M_B = -19.3$), NGC 3198 ($M_B = -19.4$) and NGC 6503 ($M_B = -18.7$). In the top panel, the rotation curves are expressed in kpc, in the bottom panel the rotation curves are scaled with their scale lengths, and normalized with the rotation velocity at two disk scale lengths.

The other extreme for the contribution of the stellar disk to the rotation curve is to assume that its contribution is negligible. The dark halo parameters for this minimum disk fit are listed in Table 2. High central densities of dark matter and small core radii are required to explain the observed steep rise in the HRCs. From Fig. 3 it is clear that the minimum disk mass models fit the rotation curves equally well as the maximum disk models. In fact, a good fit can be obtained with any mass-to-light ratio lower than the maximum disk mass-to-light ratio, demonstrating that the degeneracy that exists in the mass modeling for HSB galaxies (e.g. van Albada et al. 1985) also exists for LSB galaxies. Irrespective of the contribution of the stellar disk to the rotation curve, the similarity between the shapes of the observed rotation curves and those of the stellar

disks implies that the total mass density and the luminous mass density are coupled within the region of the optical disk.

5. DISCUSSION

The HRCs derived for the LSB galaxies rise steeply in the inner parts, and reach a flat part beyond about two disk scale lengths, as is found for HSB galaxies. In Fig. 4, the rotation curves for LSB galaxies (dotted lines) are compared with those of three typical late-type HSB galaxies from Begeman (1987), NGC 2403, NGC 3198 and NGC 6503. All the galaxies in Fig. 4 have no bulges, or only weak ones. In the top panel of Fig. 4 the radii are given in kpc. In these units, the rotation curves of LSB galaxies rise more slowly than those of HSB galaxies, indicating that these galaxies not only have lower central surface brightnesses, but also lower central mass densities, as was found by de Blok & McGaugh (1996) as well.

A different picture emerges in the bottom panel of Fig. 4, in which the rotation curves are scaled by their optical disk scale lengths and normalized to the velocity at two disk scale lengths. The normalization probably does not introduce systematic effects because the maximum difference in absolute magnitude between the galaxies in Fig. 4 is only 1.5 mag. With radii expressed in disk scale lengths, the rotation curves of the LSB galaxies presented here and those of HSB galaxies have almost identical shapes. This is consistent with the concept of a ‘universal rotation curve’ (Persic, Salucci, & Stel 1996, see also Rubin et al. 1985).

The similarity between the LSB and HSB rotation curve shapes suggests that rotation curve shapes are linked to the distribution of light in the stellar disks, independent of central disk surface brightness. Although such a link is most easily understood if the stellar disks are close to maximal, independent of surface brightness, the required high mass-to-light ratios seem to favor a picture in which LSB galaxies are dominated by dark matter within the optical disk, and HSB galaxies more by the stellar disk. The relative contribution of the stellar disk to the rotation curve may change continuously from LSB to HSB, or perhaps LSB and HSB galaxies constitute discrete galaxy families, as has been suggested by Tully & Verheijen (1997).

We thank Roelof Bottema for valuable discussions, and Erwin de Blok for making available the H I data and for useful comments. RS thanks IPAC for its hospitality during his visits which were funded in part by a grant to BFM as part of the NASA Long-Term Space Astrophysics Program.

REFERENCES

Bosma, A. 1978, PhD thesis, Rijksuniversiteit Groningen
 Bosma, A. 1981a, AJ, 86, 1791
 Bosma, A. 1981b, AJ, 86, 1825
 Begeman, K. 1987, PhD thesis, Rijksuniversiteit Groningen
 Dalcanton, J. J., Spergel, D. N., & Summers, F. J. 1997, ApJ, 482, 659
 de Blok, W. J. G., & McGaugh, S. S. 1996, ApJ, 469, L89
 de Blok, W. J. G., & McGaugh, S. S. 1997, MNRAS, 290, 533 (BM)
 de Blok, W. J. G., van der Hulst, J. M., & Bothun, G. D. 1995, MNRAS, 274, 235
 de Blok, W. J. G., McGaugh, S. S., & van der Hulst, J. M. 1996, MNRAS, 283, 18 (BMH)
 Hernandez, X., & Gilmore, G. 1998, MNRAS, 294, 595
 Kalnajs, A. J. 1983, in Internal Kinematics of Galaxies, IAU Symp. 100, ed. E. Athanassoula (Dordrecht: Reidel), 87
 Kent, S. M. 1986, AJ, 91, 1301
 Kravtsov, A. V., Klypin, A. A., Bullock, J. S., & Primack, J. R. ApJ, 502, 48
 McGaugh, S. S., & de Blok, W. J. G. 1998, ApJ, 499, 41
 Mihos, J. C., McGaugh, S. S., & de Blok, W. J. G. 1997, ApJ, 477, L79
 Persic, M., Salucci, P., & Stel, F. 1996, MNRAS, 281, 27
 Pickering, T. E., Impey, C. D., van Gorkom, J. H., & Bothun, G. D. 1997, AJ, 114, 1858
 Pfenniger, D., Combes, F., & Martinet, L. 1994, A&A, 285, 79
 Rubin, V. C., Ford, W. K., & Thonnard, N. 1978, ApJ, 225, L107
 Rubin, V. C., Ford, W. K., & Thonnard, N. 1980, ApJ, 238, 471
 Rubin, V. C., Burstein, D., Ford, Jr., W. K., & Thonnard, N. 1985, ApJ, 289, 81
 Swaters, R.A., 1999, PhD thesis, Rijksuniversiteit Groningen
 Tully, R. B., & Verheijen, M. A. W. 1997, ApJ, 484, 145
 van Albada, T. S., Bahcall, J. N., Begeman, K., & Sancisi, R. 1985, ApJ, 295, 305
 Worthey, G. 1994, ApJS, 95, 107